AN IMPETUS-STRICTION SIMULATION OF THE DYNAMICS OF AN ELASTICA

Donald J. Dichmann [1] and John H. Maddocks [2]
Institute for Physical Science and Technology
and Department of Mathematics
University of Maryland
College Park, MD 20742

To appear J. Nonlinear Science V. 6 1996

Abstract

This article concerns the three-dimensional, large deformation dynamics of an inextensible, unshearable rod. To enforce the conditions of inextensibility and unshearability, a technique we call the impetus-striction method is exploited to reformulate the constrained Lagrangian dynamics as an unconstrained Hamiltonian system in which the constraints appear as integrals of the evolution. We here show that this impetus-striction formulation naturally leads to a numerical scheme which respects the constraints and conservation laws of the continuous system. Simulations of the dynamics of a rod that is fixed at one end and free at the other are presented.

Dedication

Juan Simo and I shared many common interests in Hamiltonian systems, stability analyses, and the theory of rods. We rarely agreed on the best way of viewing problems, but we both always enjoyed debating the issues. He would undoubtedly have held strong opinions about this article, which is dedicated to him. He is sorely missed. —JHM

1 Introduction

An elastica is an inextensible, unshearable elastic rod. The inextensibility and unshearability constraints imply that the net force $\boldsymbol{n}$ acting across a cross-section is a basic unknown in the Lagrangian form of the dynamics. This net force $\boldsymbol{n}$ can be viewed as a vector of three Lagrange multipliers enforcing the constraints. A difficulty in evolving such constrained Lagrangian systems is that no time derivative of the multipliers appears in the evolution equations. The impetus-striction approach, developed in [6, 8, 19], is a method for reformulating such constrained Lagrangian systems as unconstrained Hamiltonian systems in which the constraints are manifested as integrals of motion. As is more fully explained in section 2, the impetus-striction technique is a variant of 'vakonomic' mechanics as described in [2], but with modifications tailored to a change in primary focus from ordinary differential equations subject to non-holonomic constraints, to partial differential equations subject to holonomic constraints. The impetus-striction formulation of the three-dimensional motion of an elastica was first introduced in [6, 7]. In [6, 8], this new formulation was exploited to obtain analytical stability results for solitary waves. Our purpose here is to show that the impetus-striction formulation also leads naturally to accurate numerical schemes for the computation of constrained dynamics.

[1]Research supported by the NSF, NASA GSFC and Computer Sciences Corporation
[2]Research supported by AFOSR and ONR

Our Hamiltonian formulation of rod dynamics comprises a set of fourteen nonlinear partial differential equations in one space dimension and one time dimension. The Hamiltonian also involves a set of auxiliary variables, or multipliers $\mathbf{\Lambda}(s,t)$ that we call strictions, which must be determined through a minimization procedure whenever the Hamiltonian is evaluated. In the context of unshearable, inextensible rods, the determination of the strictions involves the solution of elliptic boundary value problems that correspond, in some sense, to the limiting case of infinite wave speeds associated with compression and shear motions. Moreover, the force $\boldsymbol{n}(s,t)$ and the strictions $\mathbf{\Lambda}(s,t)$ are related through $\mathbf{\Lambda}_t = \boldsymbol{n}$. As a consequence of this identity, we demonstrate that pointwise evaluation of the strictions $\mathbf{\Lambda}$ arises in an invariant of the motion for rod dynamics related to linear momentum. Thus, although striction is an unfamiliar quantity, it does have a natural physical interpretation in the context of rod dynamics.

To numerically approximate the rod dynamics, we adopt a method of lines approach in which we first discretize the constrained Lagrangian with respect to arc-length to obtain a differential-algebraic system involving second order ordinary differential equations. We then apply the impetus-striction method to obtain an equivalent unconstrained first order Hamiltonian system of ordinary differential equations in which the spatially discretized constraints are integrals. The resulting equations can then be recognized as a spatial discretization of the continuous impetus-striction Hamiltonian system, but with an unusual differencing scheme that retains as many symmetries and integrals of the continuous system as possible, and which consequently has discrete versions of all of the continuous constraints. Moreover, for our problem the constraints are all quadratic in the configuration variables. The midpoint rule, which is the simplest symplectic Gaussian Runge-Kutta algorithm, is then employed in the time integration, and all of the quadratic invariants of the discretized system are thereby conserved in the discrete time evolution. Because the constraint functions are integrals of motion on the entire phase space of our Hamiltonian formulation, the choice of the midpoint rule for time integration reduces drift in the constraints. We discuss numerical simulations of the particular boundary value problem modelling the motion of a strut, that is a rod which is fixed at one end and free at the other. The numerical scheme presented here is further developed and analyzed in [9].

Numerical treatments of Hamiltonian formulations of unconstrained, i.e. shearable, extensible rod dynamics are presented by Simo et al. in [21, 22, 23]. Gonzalez & Simo [12] have investigated conservative time integration schemes for more general problems in nonlinear elasticity. Tabor & Klapper [24] and Klapper [14] describe another approach to constrained rod dynamics, but their numerical implementations are for cases where comparatively large dissipation is incorporated. In this article, our focus is on the conservative, constrained dynamics of inextensible and unshearable rods. As previously remarked, after the Lagrangian version of the partial differential equations in our model are discretized in space, a system of differential-algebraic equations is obtained.

The numerical solution of differential-algebraic equations is itself an active area of research. For example, numerical treatments of constrained Lagrangian and Hamiltonian dynamics are discussed in [4, 11, 16, 17], and the impetus-striction formulation can be regarded as an alternative to these methods.

In addition to the novelty of the impetus-striction approach, a second unusual feature of our treatment is the use of Euler parameters to represent the three-dimensional orientation of each cross-section of the rod. Euler parameters are now widely realized to be valuable in the modelling and analysis of rigid body dynamics (cf. e.g. [3, 13, 15]) but their use in continuum mechanics is not typical. In elasto-dynamics, Simo was among the first to exploit Euler parameters to model three-dimensional motions with finite strain (cf. [21, 22, 23]). Because they involve only ratios of quadratic functions, Euler parameters have significant computational advantages over Euler angles, which require the evaluation of ubiquitous trigonometric functions. A set of four Euler parameters is constrained to have unit norm, a condition which can lead to some awkwardness in numerics, but which combines naturally with our Hamiltonian formulation of constrained dynamics, and our time stepping algorithm. However the norm constraint on the Euler parameters is associated with a lack of strict convexity of the Lagrangian with respect to the generalized velocities, and is accordingly of a distinctly different nature from the imposed constraints of inextensibility and unshearability. As a consequence our treatment combines elements of the impetus-striction formulation, to handle the material constraints, with Dirac's theory of constraints (cf. e.g. [2, 10]) to handle the Euler parameter norm condition.

We begin in section 2 with an introduction to the impetus-striction method within a finite-dimensional context. In section 3 we summarize a generic model for the mechanics of large deformations in rods. An impetus-striction formulation of the three-dimensional motion of an inextensible and unshearable rod is described in section 4, and some associated conservation laws and integrals of motion are detailed in section 5. Our numerical discretization is developed in section 6. The discretization is an elementary, low order one that is intended to demonstrate the efficacy of the impetus-striction formulation as the basis for the stable numerical integration of constrained Lagrangian dynamics, and we make no claim as to its efficiency. Lastly, some results of our numerical simulations of struts are presented in section 7.

2 The Impetus-Striction Method

The impetus-striction method is a variant of the method of 'vakonomic' mechanics, as described in [2] p. 33, with modifications designed to facilitate applications to partial differential equations. Vakonomics is a treatment of constrained motion for systems governed by ordinary differential equations associated with a constrained Lagrangian action principle. In vakonomics a system of equations is set up to determine the multipliers associated with the constraints, and subsequently a Legendre transform can be performed to pass to the Hamiltonian form of the dynamics. By contrast, in the impetus-striction approach, we immediately construct the Legendre transform of the constrained Lagrangian to obtain a pre-Hamiltonian that depends upon the multipliers, or strictions, in addition to the phase variables. In so doing, a variational principle for the strictions can be recognized. In particular if the original Lagrangian is a convex function of the generalized velocities, the constraints are enforced, and the Hamiltonian determined, by minimization of the pre-Hamiltonian over the strictions. We believe that this new approach lays bare the convexity and symmetry properties of the resulting Hamiltonian system. The variational principle for the strictions is particularly convenient in the case of Hamiltonian partial differential equations. In our analysis we restrict attention to the case of holonomic constraints. In the case of nonholonomic constraints it is known that the constrained action principle that is our starting point does not always yield the physically appropriate time dynamics.

The essential features of the impetus-striction method are as follows. For simplicity, we consider a system of ordinary differential equations and a single constraint. The extension to partial differential equations and multiple constraints required in section 4 is not difficult. For a more detailed development, see [8].

Let $L(\boldsymbol{q}, \dot{\boldsymbol{q}}) \in \boldsymbol{R}$ be a Lagrangian in which $\boldsymbol{q} \in \boldsymbol{R}^n$ represents the configuration, $\dot{\boldsymbol{q}} \in \boldsymbol{R}^n$ represents the generalized velocities, and L is strictly convex in $\dot{\boldsymbol{q}}$. We seek to determine corresponding motions $\boldsymbol{q}(\cdot)$ subject to a holonomic constraint of the form

$$f(\boldsymbol{q}(t)) = 0, \qquad \forall t \geq 0 \ . \tag{2.1}$$

The first step leading to an unconstrained Hamiltonian formulation of the dynamics is to replace the constraint (2.1) by its time derivative

$$f_{\boldsymbol{q}}(\boldsymbol{q}(t)) \cdot \dot{\boldsymbol{q}}(t) = 0, \qquad \forall t \geq 0 \ . \tag{2.2}$$

If the initial data $\boldsymbol{q}(0)$ satisfy the constraint (2.1), the conditions (2.1) and (2.2) are equivalent. Now define the functional

$$\mathcal{L}(\boldsymbol{q}, \dot{\boldsymbol{q}}, \Lambda) \equiv L(\boldsymbol{q}, \dot{\boldsymbol{q}}) + \Lambda \, f_{\boldsymbol{q}}(\boldsymbol{q}) \cdot \dot{\boldsymbol{q}} \ . \tag{2.3}$$

The Lagrange multiplier Λ in (2.3) associated with the time-differentiated constraint is termed the *striction* [6, 8]. In order to obtain a Hamiltonian system associated with the Lagrangian (2.3), we define the conjugate variable

$$\boldsymbol{\gamma} \equiv \mathcal{L}_{\dot{\boldsymbol{q}}} = L_{\dot{\boldsymbol{q}}}(\boldsymbol{q}, \dot{\boldsymbol{q}}) + f_{\boldsymbol{q}}(\boldsymbol{q}) \, \Lambda \ , \tag{2.4}$$

and the classic (conjugate) momentum

$$\boldsymbol{p} \equiv L_{\dot{\boldsymbol{q}}}(\boldsymbol{q}, \dot{\boldsymbol{q}}) \ , \tag{2.5}$$

so $\boldsymbol{\gamma}$ and $\boldsymbol{p}$ are related by

$$\boldsymbol{p} = \boldsymbol{\gamma} - f_{\boldsymbol{q}}(\boldsymbol{q})\,\Lambda\,. \tag{2.6}$$

(To simplify notation, we have identified the derivatives $L_{\dot{\boldsymbol{q}}}$ and $f_{\boldsymbol{q}}$ with the corresponding column vectors.) The conjugate variable $\boldsymbol{\gamma}$ is thus similar to, but distinct from, the momentum $\boldsymbol{p}$. To emphasize this distinction, we refer to $\boldsymbol{\gamma}$ as the *impetus.*

Given strict convexity of L with respect to $\dot{\boldsymbol{q}}$, equation (2.5) can be solved for $\dot{\boldsymbol{q}}$:

$$\dot{\boldsymbol{q}} = \boldsymbol{v}(\boldsymbol{q}, \boldsymbol{p}) = \boldsymbol{v}(\boldsymbol{q}, \boldsymbol{\gamma} - f_{\boldsymbol{q}}\,\Lambda)\ . \tag{2.7}$$

Because $\dot{\boldsymbol{q}}$ depends upon the unknown striction Λ in (2.7), a well-defined evolutionary system cannot yet be defined. Instead, we regard the Legendre transform

$$L^*(\boldsymbol{q}, \boldsymbol{p}) \equiv \boldsymbol{p} \cdot \boldsymbol{v}(\boldsymbol{q}, \boldsymbol{p}) - L(\boldsymbol{q}, \boldsymbol{v}(\boldsymbol{q}, \boldsymbol{p}))\ , \tag{2.8}$$

as defining a *pre-Hamiltonian*

$$M(\boldsymbol{q}, \boldsymbol{\gamma}, \Lambda) \equiv L^*(\boldsymbol{q}, \boldsymbol{\gamma} - f_{\boldsymbol{q}}\,\Lambda)\ . \tag{2.9}$$

The crucial step in our formulation of the unconstrained Hamiltonian system is to observe that the expression (2.6) for the momentum $\boldsymbol{p}$ in terms of $\boldsymbol{q}$ and $\boldsymbol{\gamma}$ implies

$$M_\Lambda = -f_{\boldsymbol{q}}(\boldsymbol{q}) \cdot \boldsymbol{v}(\boldsymbol{q}, \boldsymbol{p})\ . \tag{2.10}$$

Provided that (2.7) holds, the constraint (2.2) is equivalent to requiring that $M_\Lambda = 0$. Therefore, we define the striction to be that Λ which *minimizes* the pre-Hamiltonian M for specified values of $\boldsymbol{q}$ and $\boldsymbol{\gamma}$. To see that M has a unique minimizer, recall that the Legendre transform L^* is strictly convex in $\boldsymbol{p}$ when L is strictly convex in $\dot{\boldsymbol{q}}$. Thus M is strictly convex in Λ for fixed $\boldsymbol{q}$ and $\boldsymbol{\gamma}$, so a unique minimizer $\Lambda = \tilde{\Lambda}(\boldsymbol{q}, \boldsymbol{\gamma})$ exists. (If the Lagrangian is not a convex function of the velocities a stationarity condition for the strictions is obtained.)

We now define a Hamiltonian on $\boldsymbol{R}^n \times \boldsymbol{R}^n$ by

$$H(\boldsymbol{q}, \boldsymbol{\gamma}) \equiv \min_\Lambda M(\boldsymbol{q}, \boldsymbol{\gamma}, \Lambda) = M(\boldsymbol{q}, \boldsymbol{\gamma}, \tilde{\Lambda}(\boldsymbol{q}, \boldsymbol{\gamma}))\ . \tag{2.11}$$

The associated canonical Hamiltonian system yields the evolution equations:

$$\dot{\boldsymbol{q}} \;=\; H_{\boldsymbol{\gamma}}(\boldsymbol{q}, \boldsymbol{\gamma}) = \boldsymbol{v}(\boldsymbol{q}, \tilde{\boldsymbol{p}}(\boldsymbol{q}, \boldsymbol{\gamma}))\ , \tag{2.12}$$

$$\dot{\boldsymbol{\gamma}} \;=\; -H_{\boldsymbol{q}}(\boldsymbol{q}, \boldsymbol{\gamma}) \;= L_{\boldsymbol{q}}(\boldsymbol{q}, \boldsymbol{\gamma}) + \tilde{\Lambda}(\boldsymbol{q}, \boldsymbol{\gamma}) f_{\boldsymbol{q}\boldsymbol{q}}(\boldsymbol{q}) \boldsymbol{v}(\boldsymbol{q}, \tilde{\boldsymbol{p}}(\boldsymbol{q}, \boldsymbol{\gamma}))\ , \tag{2.13}$$

where $\tilde{\boldsymbol{p}}(\boldsymbol{q}, \boldsymbol{\gamma}) \equiv \boldsymbol{\gamma} - f_{\boldsymbol{q}}(\boldsymbol{q})\,\tilde{\Lambda}(\boldsymbol{q}, \boldsymbol{\gamma})$. It is perhaps not immediately apparent, but equations (2.12) and (2.13) yield the correct dynamics. Moreover, $f(\boldsymbol{q})$ is an integral of motion. Therefore, if the initial data $\boldsymbol{q}_0$ satisfy $f(\boldsymbol{q}_0) = 0$, constraint (2.1) holds for all time.

Given a motion $\boldsymbol{q}(t)$, the momentum $\boldsymbol{p}$ is completely determined by equation (2.5). By contrast, equation (2.6) implies only that the linear combination $\boldsymbol{\gamma} - f_{\boldsymbol{q}}\,\Lambda$ is determined by the motion, and individually neither the impetus $\boldsymbol{\gamma}$ nor the striction Λ is completely specified. However, once an initial value is prescribed for either $\Lambda(0)$ or $\boldsymbol{\gamma}(0)$, the impetus $\boldsymbol{\gamma}(t)$ is determined by solving the differential equation (2.13). We refer to this indeterminacy in the initial data as a *gauge freedom*. The important point is that the gauge freedom has no effect on the evolution $\boldsymbol{q}(t)$ of the configuration. Indeed, if $(\boldsymbol{q}, \boldsymbol{\gamma})$ is a solution of the Hamiltonian system, with striction $\tilde{\Lambda}(\boldsymbol{q}, \boldsymbol{\gamma})$, then for any constant Λ^*, $(\boldsymbol{q}, \boldsymbol{\gamma} + f_{\boldsymbol{q}}\,\Lambda^*)$ is also a solution, with striction $\tilde{\Lambda}(\boldsymbol{q}, \boldsymbol{\gamma}) + \Lambda^*$. In fact it is precisely this gauge freedom that generates, via Noether's Theorem, the integral $f(\boldsymbol{q})$.

3 Classical Rod Dynamics

This section provides a brief summary of the rod model that will be employed in this article. For further details, the reader is referred to [1]. We first review the kinematics and balance laws of the director theory of rods, and specify the constitutive law to be considered. We then describe the spatial kinematics of an elastica using Euler parameters.

In the director model for rod kinematics, the dependent variables are a vector function $\boldsymbol{r}(s,t) \in \boldsymbol{R}^3$ and a right-handed orthonormal frame of directors $\boldsymbol{d}_k(s,t) \in \boldsymbol{R}^3$, $k = 1, 2, 3$. The independent variables are two scalars, namely undeformed arc-length s that ranges from 0 to length ℓ, and time t. At each time t, the curve $\boldsymbol{r}(\cdot, t)$ can be interpreted as the configuration of a material line in a long, slender elastic body. The triad $\{\boldsymbol{d}_k\}$ can be interpreted as providing information concerning the orientation of the material cross-section of the rod. (See Figure 3.1.)

The kinematics of the rod are encapsulated in the relations

$$\boldsymbol{d}_k{}' = \boldsymbol{u} \times \boldsymbol{d}_k\,, \tag{3.1}$$

$$\dot{\boldsymbol{d}}_k = \boldsymbol{\omega} \times \boldsymbol{d}_k\,, \tag{3.2}$$

$$\boldsymbol{r}' = \boldsymbol{d}_3\,. \tag{3.3}$$

Here $\boldsymbol{d}_k{}'$ denotes the partial derivative with respect to arc-length s, while $\dot{\boldsymbol{d}}_k$ denotes the partial derivative with respect to t, etc. Equations (3.1) and (3.2) follow from the orthonormality of the directors $\{\boldsymbol{d}_k\}$ as functions of s and t. The components $u_k \equiv \boldsymbol{u} \cdot \boldsymbol{d}_k$ of the (Darboux) vector $\boldsymbol{u}$ are the strains associated with bending and twist, and the components $\omega_k \equiv \boldsymbol{\omega} \cdot \boldsymbol{d}_k$ of the vector $\boldsymbol{\omega}(s,t)$ can be regarded as the body components of the angular velocity of the material cross-section at s when viewed as a rigid body. We use $\underline{\boldsymbol{u}}$ to denote the set of components (u_1, u_2, u_3), and similarly let $\underline{\omega}$ denote $(\omega_1, \omega_2, \omega_3)$. Equation (3.3) expresses the condition that the rod be inextensible and unshearable. For brevity equation (3.3) is referred to henceforth as the inextensibility condition.

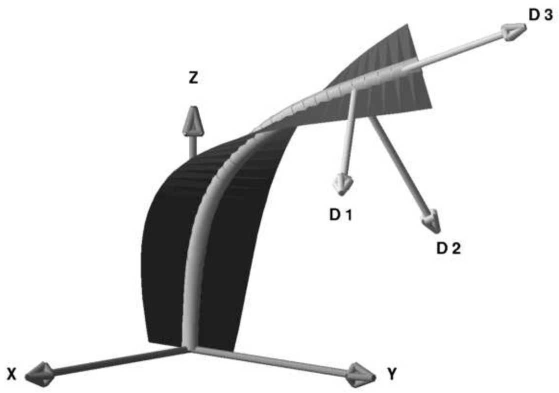

Figure 3.1: A representative ribbon describing the configuration of a rod. The centerline of the ribbon represents the centerline of the rod and is parameterized by its arc-length s. The attached ribbon illustrates the twisting of the rod. The orthogonal triad of directors $\boldsymbol{d}_1$, $\boldsymbol{d}_2$ and $\boldsymbol{d}_3$ can be thought of as indicating the orientation of a cross-section of the rod, with $\boldsymbol{d}_3$ tangent to the centerline, and $\boldsymbol{d}_1$ determining the ribbon.

The densities of linear and angular momentum are

$$\boldsymbol{p}(s,t) \equiv \rho(s)\dot{\boldsymbol{r}}(s,t)\,, \tag{3.4}$$

$$\boldsymbol{\pi}(s,t) \equiv \sum_{i,j=1}^{3} I_{ij}(s)\omega_j(s,t)\boldsymbol{d}_i(s,t)\,. \tag{3.5}$$

Here $\rho(s)$ is the mass per unit arc-length associated with the material cross-section at the point s, which is determined entirely by the reference configuration. The quantities $I_{ij}(s)$ are the components of the positive-definite inertia tensor of the material cross-section at s expressed with respect to the triad $\{\boldsymbol{d}_k\}$. It will be assumed that these inertia coefficients are independent of the strains u_k and v_k, and that $\boldsymbol{d}_1$ and $\boldsymbol{d}_2$ are the principal axes of cross-section, so that

$$I_{ij} = 0, \quad i \neq j, \qquad I_{33} = I_{11} + I_{22}\,. \tag{3.6}$$

For simplicity we will denote I_{jj} by I_j.

In a rod model the stresses acting across each material cross-section are reduced to a net force $\boldsymbol{n}(s,t)$ and moment $\boldsymbol{m}(s,t)$ (of the material on the side s^+ acting on the material on the side s^- at the point $\boldsymbol{r}(s,t)$). The balance of linear and angular momentum yield the equations

$$\dot{\boldsymbol{p}} = \boldsymbol{n}'\,, \tag{3.7}$$

and

$$\dot{\boldsymbol{\pi}} = \boldsymbol{m}' + \boldsymbol{r}' \times \boldsymbol{n}\,. \tag{3.8}$$

It is stipulated that the constraint (3.3) holds for all possible forces and moments. The force is determined by this requirement, and a constitutive equation is specified only for the moments. We assume the unstressed rod is straight with no twist, and the components $m_j \equiv \boldsymbol{m} \cdot \boldsymbol{d}_j$ to be given by the linear constitutive relations

$$m_i = K_i u_i \,. \tag{3.9}$$

More general reference configurations and hyperelastic constitutive relations could also be considered in a straightforward manner. The kinetic energy of the rod is given by

$$T(\boldsymbol{r}, \underline{\omega}) = \int_0^\ell \frac{1}{2} \left\{ \rho |\boldsymbol{r}_t|^2 + \sum_{j=1}^{3} I_j \omega_j^2 \right\} ds \,, \tag{3.10}$$

and the potential energy is

$$V(\underline{\boldsymbol{u}}) = \int_0^\ell \frac{1}{2} K_j u_j^2 \, ds \,. \tag{3.11}$$

We must specify the set of boundary conditions which the rod is to satisfy. In this article, we consider a strut, that is a rod with one end held fixed and the other end free. Specifically, the end $s = 0$ is fixed at the origin with the directors aligned with a reference frame $\{\boldsymbol{e}_k\}$, so that

$$\boldsymbol{r}(0,t) = \boldsymbol{0} \,, \tag{3.12}$$

and

$$\boldsymbol{d}_k(0,t) = \boldsymbol{e}_k \,. \tag{3.13}$$

The end $s = \ell$ experiences no loads, so that

$$\boldsymbol{n}(\ell,t) = \boldsymbol{0} \,, \qquad \boldsymbol{m}(\ell,t) = \boldsymbol{0} \,. \tag{3.14}$$

To fully describe the three-dimensional motion of a rod, it is convenient to parametrize the directors $\{\boldsymbol{d}_k\}$, which is equivalent to selecting a representation for the group of proper orthogonal transformations $SO(3)$. Euler parameters provide a four-dimensional, global, two-to-one parametrization of $SO(3)$ which involves only ratios of quadratic functions. A set of Euler parameters, also called a unit quaternion, is a quadruple of real numbers $\boldsymbol{q} = (q_1, q_2, q_3, q_4)^T$ that satisfies the identity

$$\boldsymbol{q} \cdot \boldsymbol{q} = {q_1}^2 + {q_2}^2 + {q_3}^2 + q_4^2 = 1 \,. \tag{3.15}$$

By definition, the Euler parameters associated with a rotation through an angle Φ about an axis determined by a unit vector $\boldsymbol{k} = k_j \boldsymbol{e}_j$ are given by $q_j = k_j \sin(\Phi/2)$ for $j = 1, 2, 3$, and $q_4 = \cos(\Phi/2)$. The set of directors $\{\boldsymbol{d}_1, \boldsymbol{d}_2, \boldsymbol{d}_3\}$ can be expressed in terms of the Euler parameters as

$$\boldsymbol{d}_1(\boldsymbol{q}) = \begin{pmatrix} q_1^2 - q_2^2 - q_3^2 + q_4^2 \\ 2(q_1 q_2 + q_3 q_4) \\ 2(q_1 q_3 - q_2 q_4) \end{pmatrix} , \tag{3.16}$$

$$\boldsymbol{d}_2(\boldsymbol{q}) = \begin{pmatrix} 2(q_1q_2 - q_3q_4) \\ -q_1^2 + q_2^2 - q_3^2 + q_4^2 \\ 2(q_1q_4 + q_2q_3) \end{pmatrix}, \tag{3.17}$$

$$\boldsymbol{d}_3(\boldsymbol{q}) = \begin{pmatrix} 2(q_1q_3 + q_2q_4) \\ 2(q_2q_3 - q_1q_4) \\ -q_1^2 - q_2^2 + q_3^2 + q_4^2 \end{pmatrix}. \tag{3.18}$$

In particular the set of Euler parameters

$$\boldsymbol{q}(0,t) = (0,0,0,1)^T \tag{3.19}$$

satisfies the boundary conditions (3.13).

The strains $\boldsymbol{u}$ and the angular velocities $\boldsymbol{\omega}$ are given in terms of the Euler parameters by

$$u_j = \frac{2\boldsymbol{q}_s \cdot \boldsymbol{B}_j \boldsymbol{q}}{|\boldsymbol{q}|^2}, \qquad j = 1,2,3, \tag{3.20}$$

and

$$\omega_j = \frac{2\boldsymbol{q}_t \cdot \boldsymbol{B}_j \boldsymbol{q}}{|\boldsymbol{q}|^2}, \qquad j = 1,2,3, \tag{3.21}$$

where $\{\boldsymbol{B}_1, \boldsymbol{B}_2, \boldsymbol{B}_3\}$ is a set of three 4-by-4 skew matrices, satisfying the relations

$$\boldsymbol{B}_1\boldsymbol{q} = \begin{pmatrix} q_4, & q_3, & -q_2, & -q_1 \end{pmatrix}^T, \tag{3.22}$$

$$\boldsymbol{B}_2\boldsymbol{q} = \begin{pmatrix} -q_3, & q_4, & q_1, & -q_2 \end{pmatrix}^T, \tag{3.23}$$

$$\boldsymbol{B}_3\boldsymbol{q} = \begin{pmatrix} q_2, & -q_1, & q_4, & -q_3 \end{pmatrix}^T. \tag{3.24}$$

The skewness of the matrices $\boldsymbol{B}_j$ together with the norm constraint (3.15) imply that the four vectors $\{\boldsymbol{q}, \boldsymbol{B}_1\boldsymbol{q}, \boldsymbol{B}_2\boldsymbol{q}, \boldsymbol{B}_3\boldsymbol{q}\}$ form an orthonormal basis for $\boldsymbol{R}^4$. Geometrically, the vector $\boldsymbol{B}_j\boldsymbol{q}$ acts as the infinitesimal generator of rotation about the $\boldsymbol{d}_j$ axis.

4 Hamiltonian Formulation

We now obtain a Hamiltonian formulation describing the three-dimensional motion of an inextensible and unshearable rod, represented in terms of Euler parameters. For the partial differential equations describing rod dynamics, we must deal with both the Euler parameter constraint and the more complicated inextensibility and unshearability constraints. It is because of these constraints that we adopt the impetus-striction formulation.

The time derivative of the inextensibility constraint (3.3) is

$$(\boldsymbol{r}_s - \boldsymbol{d}_3)_t = \boldsymbol{r}_{st} - \boldsymbol{D}_3(\boldsymbol{q})^T \boldsymbol{q}_t = \boldsymbol{0}, \tag{4.1}$$

where, for $k = 1,2,3$, the 3-by-4 matrices $\boldsymbol{D}_k(\boldsymbol{q})$ are

$$\boldsymbol{D}_k(\boldsymbol{q}) \equiv \left(\frac{\partial \boldsymbol{d}_k}{\partial \boldsymbol{q}}\right)^T = \frac{2}{|\boldsymbol{q}|^2} \sum_{i,j=1}^{3} \epsilon_{ijk} \boldsymbol{B}_j \boldsymbol{q} \otimes \boldsymbol{d}_i + \frac{2}{|\boldsymbol{q}|^2} \boldsymbol{q} \otimes \boldsymbol{d}_k, \tag{4.2}$$

with $\otimes$ denoting the outer product. (A direct differentiation of equations (3.16)–(3.18) yields a simpler expression for the matrices $\boldsymbol{D}_k(\boldsymbol{q})$, but equation (4.2) has proved to be a more useful form for analysis.) The time derivative of equation (3.15) is

$$\boldsymbol{q} \cdot \boldsymbol{q}_t = 0. \tag{4.3}$$

Consequently, the Lagrangian we consider is

$$\begin{aligned}
\mathcal{L} &= T(\boldsymbol{r}, \underline{\omega}) - V(\underline{\boldsymbol{u}}) + \int_0^\ell \left\{\Lambda \cdot \left(\boldsymbol{r}_{st} - \boldsymbol{D}_3(\boldsymbol{q})^T \boldsymbol{q}_t\right) + \nu \boldsymbol{q} \cdot \boldsymbol{q}_t\right\} ds\,, \\
&= \int_0^\ell \left\{\frac{1}{2}\rho|\boldsymbol{r}_t|^2 + \frac{1}{2}\sum_{j=1}^{3} I_j \omega_j^2 - \frac{1}{2}\sum_{j=1}^{3} K_j u_j^2 + \boldsymbol{\Lambda} \cdot \boldsymbol{r}_{st} - \boldsymbol{q}_t \cdot \boldsymbol{D}_3(\boldsymbol{q})\boldsymbol{\Lambda} + \nu \boldsymbol{q} \cdot \boldsymbol{q}_t\right\} ds\,,
\end{aligned} \tag{4.4}$$

where the kinetic energy T is given by (3.10), the potential energy V is given by (3.11), the angular velocities ω_j are given by (3.21) the strains u_j are given by (3.20), and $\boldsymbol{\Lambda}$ and ν are the Lagrange multipliers associated respectively with the constraints (4.1) and (4.3). It can be shown that the striction $\boldsymbol{\Lambda}$ appearing in (4.4) is the time anti-derivative of the force $\boldsymbol{n}$, that is

$$\boldsymbol{\Lambda}_t = \boldsymbol{n} \tag{4.5}$$

(cf. [6]). The impetuses associated with translation and rotation are defined by

$$\boldsymbol{\chi} \equiv \frac{\partial \mathcal{L}}{\partial \boldsymbol{r}_t} = \rho \boldsymbol{r}_t - \boldsymbol{\Lambda}_s\,, \tag{4.6}$$

$$\boldsymbol{\gamma} \equiv \frac{\partial \mathcal{L}}{\partial \boldsymbol{q}_t} = \sum_{j=1}^{3} I_j \omega_j \frac{2\boldsymbol{B}_j \boldsymbol{q}}{|\boldsymbol{q}|^2} - \boldsymbol{D}_3(\boldsymbol{q})\boldsymbol{\Lambda} + \nu \boldsymbol{q}\,. \tag{4.7}$$

Combining equations (3.4) and (4.6), we can rewrite the linear momentum density as

$$\boldsymbol{p} = \rho \boldsymbol{r}_t = \boldsymbol{\chi} + \boldsymbol{\Lambda}_s\,. \tag{4.8}$$

One can use the orthonormality of the basis $\{\boldsymbol{q}, \boldsymbol{B}_j \boldsymbol{q}\}$, together with the constraint (4.3), to solve equation (4.7) for the multiplier ν and the components $\pi_j = \boldsymbol{\pi} \cdot \boldsymbol{d}_j$ of angular momentum density to obtain

$$\pi_j = I_j \omega_j = \tfrac{1}{2}\boldsymbol{\gamma} \cdot \boldsymbol{B}_j \boldsymbol{q} + \sum_{i=1}^{3} \epsilon_{ij3}\, \boldsymbol{d}_i \cdot \boldsymbol{\Lambda} = \tfrac{1}{2}\boldsymbol{\gamma} \cdot \boldsymbol{B}_j \boldsymbol{q} + \boldsymbol{d}_j \cdot (\boldsymbol{d}_3 \times \boldsymbol{\Lambda}) \tag{4.9}$$

and

$$\nu = [\boldsymbol{\gamma} + \boldsymbol{D}_3(\boldsymbol{q})\boldsymbol{\Lambda}] \cdot \frac{\boldsymbol{q}}{|\boldsymbol{q}|^2} = \frac{\boldsymbol{\gamma} \cdot \boldsymbol{q}}{|\boldsymbol{q}|^2} + 2\boldsymbol{d}_3 \cdot \boldsymbol{\Lambda}\,, \tag{4.10}$$

where the second equality in (4.10) follows from the expression (4.2) for $\boldsymbol{D}_3(\boldsymbol{q})$. We can then employ the orthonormality of the basis $\{\boldsymbol{q}, \boldsymbol{B}_j \boldsymbol{q}\}$ to invert equation (3.21) for the angular velocities and obtain the expression for $\boldsymbol{q}_t$, namely

$$\boldsymbol{q}_t = \sum_{j=1}^{3} \tfrac{1}{2}\omega_j \boldsymbol{B}_j \boldsymbol{q}\,, \tag{4.11}$$

where now ω_j is to be interpreted as being defined in terms of the Hamiltonian variables by (4.9).

It is necessary to invoke the constraint (4.3) in order to solve (4.7) for $\boldsymbol{q}_t$, for otherwise the component $\boldsymbol{q} \cdot \boldsymbol{q}_t$ is indeterminate. This is a special case of a general theory developed by Dirac [10], which constructs Hamiltonian formulations of Lagrangian systems that are not strictly convex in the velocities. The Dirac theory, and particularly associated gauge freedoms, remains an active area of research (cf. [5] and references therein). Notice that in contrast to the striction $\boldsymbol{\Lambda}$, the multiplier ν does not appear in the expressions (4.8) and (4.9) for $\boldsymbol{p}$ and π_j. As a consequence, ν does not arise in the Hamiltonian dynamics.

The next step in our Hamiltonian formulation is to express the total energy, which is the sum of the kinetic and potential energies, in terms of the Hamiltonian state variable $\boldsymbol{z} = (\boldsymbol{r}, \boldsymbol{q}, \boldsymbol{\chi}, \boldsymbol{\gamma})$. Equations (4.8) and (4.9) allow us to rewrite the energy in the form of the pre-Hamiltonian

$$M(\boldsymbol{z}, \boldsymbol{\Lambda}) = \int_0^\ell \frac{1}{2} \left\{ \rho^{-1} |\boldsymbol{p}|^2 + \sum_{j=1}^{3} I_j^{-1} \pi_j^2 + \sum_{j=1}^{3} K_j u_j^2 \right\} ds \,, \tag{4.12}$$

where the linear momentum density $\boldsymbol{p}$ is given by (4.8), the components of angular momentum density π_j are given by (4.9), and the components of strain u_j are given by (3.20). The strictions are determined by the requirement that $\boldsymbol{\Lambda} = \tilde{\boldsymbol{\Lambda}}(\boldsymbol{z})$ minimize M for given phase $\boldsymbol{z} = (\boldsymbol{r}, \boldsymbol{q}, \boldsymbol{\chi}, \boldsymbol{\gamma})$, so the strictions satisfy $\delta M / \delta \boldsymbol{\Lambda} = \mathbf{0}$, or

$$\mathbf{0} = - \left[\rho^{-1} (\boldsymbol{\chi} + \boldsymbol{\Lambda}_s) \right]_s - I_1^{-1} \left(\tfrac{1}{2} \boldsymbol{\gamma} \cdot \boldsymbol{B}_1 \boldsymbol{q} - \boldsymbol{d}_2 \cdot \boldsymbol{\Lambda} \right) \boldsymbol{d}_2 + I_2^{-1} \left(\tfrac{1}{2} \boldsymbol{\gamma} \cdot \boldsymbol{B}_2 \boldsymbol{q} + \boldsymbol{d}_1 \cdot \boldsymbol{\Lambda} \right) \boldsymbol{d}_1 \,. \tag{4.13}$$

The boundary conditions connected with the set of elliptic equations (4.13) are the natural boundary condition

$$(\boldsymbol{\chi} + \boldsymbol{\Lambda}_s)(0, t) = \mathbf{0} \,, \tag{4.14}$$

corresponding to the fact that the end $s = 0$ is fixed, and

$$\boldsymbol{\Lambda}(\ell, t) = \mathbf{0} \,, \tag{4.15}$$

corresponding to the fact that the end $s = \ell$ is free. Using equations (4.8) and (4.9), one can show that the equation (4.13) is simply the enforcement of the inextensibility constraint. The striction $\tilde{\boldsymbol{\Lambda}}(\boldsymbol{z})$ is uniquely determined by equations (4.13) – (4.15). The proof that the striction $\tilde{\boldsymbol{\Lambda}}$ exists and is unique is given in [8] for planar motions (of an infinite rod), and in [6] for three-dimensional motion.

Henceforth we shall use $\boldsymbol{p}$, π_j and ω_j respectively to denote the linear momentum density, the components of angular momentum density and the components of angular velocity, each evaluated at $\boldsymbol{\Lambda} = \tilde{\boldsymbol{\Lambda}}(\boldsymbol{z})$. The resulting Hamiltonian is

$$H(\boldsymbol{z}) = M(\boldsymbol{z}, \tilde{\boldsymbol{\Lambda}}(\boldsymbol{z})) = \int_0^\ell \frac{1}{2} \left\{ \rho^{-1} |\boldsymbol{p}|^2 + \sum_{j=1}^{3} I_j^{-1} \pi_j^2 + \sum_{j=1}^{3} K_j u_j^2 \right\} ds \,, \tag{4.16}$$

with the associated Hamiltonian system of partial differential equations

$$\boldsymbol{r}_t = \frac{\delta H}{\delta \boldsymbol{\chi}} = \rho^{-1}\boldsymbol{p}\,, \tag{4.17}$$

$$\boldsymbol{q}_t = \frac{\delta H}{\delta \boldsymbol{\gamma}} = \sum_{j=1}^{3} \tfrac{1}{2}\omega_j \boldsymbol{B}_j \boldsymbol{q}\,, \tag{4.18}$$

$$\boldsymbol{\chi}_t = -\frac{\delta H}{\delta \boldsymbol{r}} = \boldsymbol{0}\,, \tag{4.19}$$

$$\begin{aligned}\boldsymbol{\gamma}_t = -\frac{\delta H}{\delta \boldsymbol{q}} &= \sum_{j=1}^{3}\omega_j\left(\tfrac{1}{2}\boldsymbol{B}_j\boldsymbol{\gamma} - \sum_{i=1}^{3}\epsilon_{ij3}\boldsymbol{D}_i\,\tilde{\boldsymbol{\Lambda}}\right)\\ &\quad + \sum_{j=1}^{3}\left[K_j u_j \frac{2\boldsymbol{B}_j\boldsymbol{q}}{|\boldsymbol{q}|^2}\right]_s + \sum_{j=1}^{3} K_j u_j \frac{2\boldsymbol{B}_j\boldsymbol{q}_s}{|\boldsymbol{q}|^2} + \sum_{j=1}^{3} K_j u_j^2 \frac{2\boldsymbol{q}}{|\boldsymbol{q}|^2}\,.\end{aligned} \tag{4.20}$$

The dynamics (4.17) – (4.20) are subject to the boundary conditions (3.12) and (3.19). To determine the initial conditions, one must fix the gauge by specifying $\tilde{\boldsymbol{\Lambda}}(s,0)$ and $\nu(s)$. It is convenient to set

$$\tilde{\boldsymbol{\Lambda}}(s,0) = \boldsymbol{0}\,, \tag{4.21}$$

$$\nu(s) = \boldsymbol{0}\,, \tag{4.22}$$

which satisfy the boundary condition (4.15). Equations (4.21) and (4.22) together with definitions (4.6) and (4.7) yield the initial conditions for the impetuses,

$$\boldsymbol{\chi}(s,0) = \rho(s)\boldsymbol{r}_t(s,0)\,, \tag{4.23}$$

$$\boldsymbol{\gamma}(s,0) = \sum_{j=1}^{3} I_j(s)\omega_j(s,0)\frac{2\boldsymbol{B}_j\boldsymbol{q}(s,0)}{|\boldsymbol{q}(s,0)|^2}\,. \tag{4.24}$$

5 Conservation Laws and Integrals of Motion

A number of conservation laws and integrals of motion arise in our model of the rod dynamics. The Lagrangian forms of these conservation laws are discussed in detail in [18]. Whether these conservation laws imply associated integrals of motion depends upon the boundary conditions under consideration. For example, the Hamiltonian system is time-independent, and the Hamiltonian is an integral of motion. On the other hand, the balance law (3.7) for linear momentum is a conservation law, but for the boundary conditions (3.12) – (3.14) appropriate for a strut, the total linear momentum

$$\boldsymbol{P}(t) \equiv \int_0^\ell \boldsymbol{p}(s,t)\,ds \tag{5.1}$$

is not an integral of motion.

The Hamiltonian system under consideration also possesses several pointwise invariants. By the impetus-striction construction, the quantities $|\boldsymbol{q}(s,t)|^2$ and $\boldsymbol{r}_s(s,t) - \boldsymbol{d}_3(s,t)$ appearing in the constraints are integrals of motion for each s. Moreover, the variable $\boldsymbol{r}$ is ignorable (i.e., the

Hamiltonian does not depend upon $\boldsymbol{r}$), so its conjugate variable, namely the impetus $\boldsymbol{\chi}$, is also a pointwise invariant.

Although the total linear momentum is not conserved for the strut, the pointwise invariance of the impetus trivially implies that the total linear impetus

$$\boldsymbol{X}(t) \equiv \int_0^{\ell} \boldsymbol{\chi}(s,t)\, ds \tag{5.2}$$

is also conserved. The expressions (4.8) and (5.1) for the linear momentum density and total linear momentum together with the boundary condition (4.15) can be used to rewrite the total linear impetus as

$$\boldsymbol{X}(t) = \boldsymbol{P}(t) + \tilde{\boldsymbol{\Lambda}}(0,t)\,. \tag{5.3}$$

Equation (5.3) illustrates the physical meaning of the strictions within the context of rods: The change in $\tilde{\boldsymbol{\Lambda}}(0,\cdot)$ over the time interval $[0,t]$ is the negative of the change in the linear momentum of the rod over the same time interval. The negative sign appearing in this interpretation is merely a consequence of the sign convention for $\boldsymbol{\Lambda}$ in our definition of the Lagrangian (4.4). More generally, because $\boldsymbol{\chi}(s,t)$ is constant for each s, it follows that for any a and b such that $0 \leq a < b \leq \ell$, the quantity

$$\int_a^b \boldsymbol{p}(s,t)\, ds - \tilde{\boldsymbol{\Lambda}}(b,t) + \tilde{\boldsymbol{\Lambda}}(a,t) \tag{5.4}$$

is conserved, so the change in $\tilde{\boldsymbol{\Lambda}}(b,\cdot) - \tilde{\boldsymbol{\Lambda}}(a,\cdot)$ over the time interval $[0,t]$ is the the change in the linear momentum of the segment $[a,b]$ over the same time interval. This interpretation of the striction is equivalent to the statement (4.5) that the striction $\boldsymbol{\Lambda}$ is the time anti-derivative of the force $\boldsymbol{n}$ in the context of rods. One could exploit the gauge freedom in the choice of initial data to specify $\boldsymbol{\chi}(s,0) = 0$ for all s, and so guarantee that the quantity $\tilde{\boldsymbol{\Lambda}}(b,t) - \tilde{\boldsymbol{\Lambda}}(a,t)$ actually equals the linear momentum of the segment $[a,b]$, for all a, b and for all times t. It is reasonable to regard (5.3) as an integral of motion because it is expressed in terms of quantities that are determined solely by the location in phase space.

6 Numerical Approximation of the Hamiltonian Dynamics

We now shift our focus to the numerical integration of our model equations. Our purpose here is to demonstrate the feasibility of the impetus-striction method as the basis for a stable numerical integration scheme for constrained systems, and in the first instance no efforts were made to optimize the speed of the code. To numerically approximate the partial differential equations arising in our model of rod dynamics we employ the method of lines and first discretize with respect to arc-length, thereby obtaining a system of ordinary differential equations. This first stage is referred to as the semi-discretization. The second stage is then to numerically integrate the system of ordinary differential equations in time.

At both stages, our choice of discretization has been guided by two goals. First, we retain the Hamiltonian structure of the equations. Second, we preserve, as much as is possible, the conservation laws and invariants of the original system of partial differential equations. In particular, we enforce discrete versions of inextensibility condition (3.3), and norm condition (3.15) on the Euler parameters. To achieve these goals, it is simplest to discretize the constrained Lagrangian with respect to arc-length s, and then to apply the impetus-striction method to obtain a Hamiltonian system of ordinary differential equations that can also be recognized as a discretization of the Hamiltonian partial differential equations. In section 1 we describe a finite-difference scheme which is second order in space, and in section 2 we motivate the choice of the midpoint rule as our time-stepping scheme.

6.1 Spatial Discretization

Our first step is to discretize the rod with respect to arc-length over a uniform grid $\{s^n\}$, where n runs from 0 to N, to obtain N segments of length $h \equiv \ell/N$. The segments are numbered by half-integers, running from $\frac{1}{2}$ to $(N-\frac{1}{2})$, with segment $(n+\frac{1}{2})$ lying between the nodes n and $n+1$. We find it convenient to associate a position $\boldsymbol{r}^n$ with each node n, but to associate a quaternion $\boldsymbol{q}^{n+\frac{1}{2}}$ with each segment $(n+\frac{1}{2})$. In this way, a $O(h^2)$ discrete form of the inextensibility condition (3.3) can be written as

$$\frac{\boldsymbol{r}^{n+1} - \boldsymbol{r}^n}{h} = \boldsymbol{d}_3^{n+\frac{1}{2}} , \tag{6.1.1}$$

where

$$\boldsymbol{d}_j^{n+\frac{1}{2}} \equiv \boldsymbol{d}_j(\boldsymbol{q}^{n+\frac{1}{2}}) , \tag{6.1.2}$$

and the norm condition on the quaternions is

$$\boldsymbol{q}^{n+\frac{1}{2}} \cdot \boldsymbol{q}^{n+\frac{1}{2}} = 1 . \tag{6.1.3}$$

Each segment has an associated striction and multiplier arising from the inextensibility and norm conditions, denoted $\boldsymbol{\Lambda}^{n+\frac{1}{2}}$ and $\nu^{n+\frac{1}{2}}$ respectively. The discrete analogs of the boundary conditions (3.12) and (3.19) are

$$\boldsymbol{r}^0(t) = \boldsymbol{0}, \tag{6.1.4}$$

and

$$\tfrac{1}{2}\left(\boldsymbol{q}^{\frac{1}{2}}(t) + \boldsymbol{q}^{-\frac{1}{2}}(t)\right) = (0,0,0,1)^T . \tag{6.1.5}$$

Here (6.1.5) is a second-order approximation to (3.19) involving the additional variable $\boldsymbol{q}^{-\frac{1}{2}}(t)$ which also appears in the discretization of the strain u_j^n.

By using the trapezoid rule for variables defined at nodes, and the midpoint rule for variables associated with segments, the continuous Lagrangian (4.4) can be approximated to order $O(h^2)$ by the discretized Lagrangian

$$
\begin{aligned}
\mathcal{L}^N(\boldsymbol{q},\boldsymbol{r},\boldsymbol{\Lambda},\nu) \;=\; & \sum_{n=1}^{N-1}\frac{1}{2}\rho^n|\dot{\boldsymbol{r}}^n|^2+\frac{\rho^N}{4}|\dot{\boldsymbol{r}}^N|^2+\sum_{n=0}^{N-1}\sum_{j=1}^{3}\frac{1}{2}I_j^{n+\frac{1}{2}}\left(\omega_j^{n+\frac{1}{2}}\right)^2 \\
& -\sum_{j=1}^{3}\frac{K_j^0}{4}\left(u_j^0\right)^2-\sum_{n=1}^{N-1}\sum_{j=1}^{3}\frac{1}{2}K_j^n\left(u_j^n\right)^2 \\
& +\sum_{n=0}^{N-1}\boldsymbol{\Lambda}^{n+\frac{1}{2}}\cdot\left[\frac{\dot{\boldsymbol{r}}^{n+1}-\dot{\boldsymbol{r}}^n}{h}-\left(\boldsymbol{D}_3^{n+\frac{1}{2}}\right)^T\dot{\boldsymbol{q}}^{n+\frac{1}{2}}\right] \\
& +\sum_{n=0}^{N-1}\nu^{n+\frac{1}{2}}\boldsymbol{q}^{n+\frac{1}{2}}\cdot\dot{\boldsymbol{q}}^{n+\frac{1}{2}}\;, \qquad (6.1.6)
\end{aligned}
$$

where the boundary conditions (6.1.4) and $u_j^N=0$ have been used,

$$
\omega_j^{n+\frac{1}{2}} \equiv \frac{2\dot{\boldsymbol{q}}^{n+\frac{1}{2}}\cdot\boldsymbol{B}_j\boldsymbol{q}^{n+\frac{1}{2}}}{|\boldsymbol{q}^{n+\frac{1}{2}}|^2}, \qquad n=0\;,\ldots,(N-1), \qquad (6.1.7)
$$

and

$$
\begin{aligned}
u_j^n \;\equiv\; & \frac{2}{|\boldsymbol{q}^{n+\frac{1}{2}}||\boldsymbol{q}^{n-\frac{1}{2}}|}\left(\frac{\boldsymbol{q}^{n+\frac{1}{2}}-\boldsymbol{q}^{n-\frac{1}{2}}}{h}\right)\cdot\boldsymbol{B}_j\left(\frac{\boldsymbol{q}^{n+\frac{1}{2}}+\boldsymbol{q}^{n-\frac{1}{2}}}{2}\right) \\
= \;& \frac{2\boldsymbol{q}^{n+\frac{1}{2}}\cdot\boldsymbol{B}_j\boldsymbol{q}^{n-\frac{1}{2}}}{h|\boldsymbol{q}^{n+\frac{1}{2}}||\boldsymbol{q}^{n-\frac{1}{2}}|}\;, \qquad n=0,\ldots,(N-1), \qquad (6.1.8)
\end{aligned}
$$

with $u_j^N=0$, and $\boldsymbol{q}^{-\frac{1}{2}}$ defined through boundary condition (6.1.5). The expression (6.1.7) is a natural semi-discrete form of equation (3.21). The expression (6.1.8) is an approximation to the strain (3.20) that is closely related to the quaternion which measures the rotation between the frame $\left\{\boldsymbol{d}^{n-\frac{1}{2}}\right\}$ and the frame $\left\{\boldsymbol{d}^{n+\frac{1}{2}}\right\}$. However this choice of the discrete approximation to the strain u_j is by no means unique.

The pre-Hamiltonian can then be written as

$$
\begin{aligned}
M^N(\boldsymbol{q},\boldsymbol{\chi},\boldsymbol{\gamma},\boldsymbol{\Lambda}) \;=\; & \sum_{n=1}^{N-1}\frac{|\boldsymbol{p}^n|^2}{2\rho^n}+\frac{|\boldsymbol{p}^N|^2}{\rho^N}+\sum_{n=0}^{N-1}\sum_{j=1}^{3}\frac{1}{2}\left(I_j^{n+\frac{1}{2}}\right)^{-1}\left(\pi_j^{n+\frac{1}{2}}\right)^2 \\
& +\sum_{j=1}^{3}\frac{K_j^0}{4}\left(u_j^0\right)^2+\sum_{n=0}^{N-1}\sum_{j=1}^{3}\frac{1}{2}K_j^n\left(u_j^n\right)^2\;. \qquad (6.1.9)
\end{aligned}
$$

Here the linear momentum density associated with each node is

$$
\boldsymbol{p}^n=\boldsymbol{\chi}^n+\frac{\boldsymbol{\Lambda}^{n+\frac{1}{2}}-\boldsymbol{\Lambda}^{n-\frac{1}{2}}}{h}, \qquad n=1,\ldots,N \qquad (6.1.10)
$$

(with $\boldsymbol{p}^0=0$ reflecting boundary condition (6.1.4)), and the components of angular momentum density associated with segment $n+\frac{1}{2}$ (for $n=0,\ldots,N$) are

$$
\pi_j^{n+\frac{1}{2}}=I_j^{n+\frac{1}{2}}\omega_j^{n+\frac{1}{2}}=\tfrac{1}{2}\boldsymbol{\gamma}^{n+\frac{1}{2}}\cdot\boldsymbol{B}_j\boldsymbol{q}^{n+\frac{1}{2}}+\boldsymbol{d}_j^{n+\frac{1}{2}}\cdot\left(\boldsymbol{d}_3^{n+\frac{1}{2}}\times\boldsymbol{\Lambda}^{n+\frac{1}{2}}\right)\;. \qquad (6.1.11)
$$

(Cf. equations (4.8) and (4.9).) The strictions $\tilde{\mathbf{\Lambda}}^{n+\frac{1}{2}}$ for $n = 0, \ldots, (N-1)$ are chosen such that the semi-discrete inextensibility condition (6.1.1) is enforced, while $\mathbf{\Lambda}^{N+\frac{1}{2}}$ is defined through the discretization

$$\tfrac{1}{2}\left(\mathbf{\Lambda}^{N+\frac{1}{2}} + \mathbf{\Lambda}^{N-\frac{1}{2}}\right) = \mathbf{0} \tag{6.1.12}$$

of boundary condition (4.15). This condition yields a system of linear equations, involving a banded, positive definite symmetric matrix, which must be solved whenever the Hamiltonian is evaluated. To specify the gauge, we employ the discrete analogs of equations (4.21) and (4.22).

Inserting the strictions $\tilde{\mathbf{\Lambda}}^{n+\frac{1}{2}}$ into the pre-Hamiltonian M (6.1.9), we obtain the Hamiltonian

$$H^N(\boldsymbol{z}) = M^N(\boldsymbol{z}, \tilde{\mathbf{\Lambda}}(\boldsymbol{z})) \ , \tag{6.1.13}$$

with associated dynamics

$$\begin{aligned}
\dot{\boldsymbol{r}}^{n+1} &= \frac{\partial H^N}{\partial \boldsymbol{\chi}^{n+1}} \, , && (6.1.14)\\
\dot{\boldsymbol{q}}^{n+\frac{1}{2}} &= \frac{\partial H^N}{\partial \boldsymbol{\gamma}^{n+\frac{1}{2}}} \, , && (6.1.15)\\
\dot{\boldsymbol{\chi}}^{n+1} &= -\frac{\partial H^N}{\partial \boldsymbol{r}^{n+1}} = \mathbf{0} \, , && (6.1.16)\\
\dot{\boldsymbol{\gamma}}^{n+\frac{1}{2}} &= -\frac{\partial H^N}{\partial \boldsymbol{q}^{n+\frac{1}{2}}} \, , && (6.1.17)
\end{aligned}$$

for $n = 0, \ldots, (N-1)$. The semi-discrete Hamiltonian system of ordinary differential equations (6.1.14) – (6.1.17) inherits versions of all but one of the conservations laws of the associated partial differential equations (4.17) – (4.20). The exception is the conservation law for linear impulse, which corresponds to the symmetry of translation in arc-length, and which is therefore lost in the spatial discretization (cf. [18], [9]). The Hamiltonian (6.1.13) is time-independent, and is therefore conserved. The semi-discrete forms of the inextensibility constraint (6.1.1) and the norm condition on quaternions (6.1.3) are conserved as a consequence of the impetus-striction formulation. The semi-discrete version of the total linear momentum, analogous to (5.2), is given by

$$\boldsymbol{P}^N(t) \equiv h\left(\sum_{n=1}^{N-1} \boldsymbol{p}^n(t) + \tfrac{1}{2}\boldsymbol{p}^N(t)\right) \ , \tag{6.1.18}$$

where $\boldsymbol{p}^n$ is given by (6.1.10). Although the total linear momentum is not conserved, the total linear impetus

$$\boldsymbol{X}^N(t) \equiv h\left(\sum_{n=1}^{N-1} \boldsymbol{\chi}^n(t) + \tfrac{1}{2}\boldsymbol{\chi}^N(t)\right) = \boldsymbol{P}^N(t) + \tilde{\mathbf{\Lambda}}^{\frac{1}{2}}(t) \, , \tag{6.1.19}$$

analogous to (5.3), is an integral of motion.

6.2 Time Discretization

Having discretized the Hamiltonian system with respect to arc-length, we must also select a method to approximate the time evolution associated with the system of ordinary differential equations (6.1.14) – (6.1.17). Our primary criteria in selecting a time integration scheme were to preserve both the Hamiltonian structure of the system, and as many of the invariants of motions as possible, but most importantly the inextensibility condition (6.1.1) and the norm condition (6.1.3).

Various integration schemes have been developed that preserve the symplectic structure of a Hamiltonian system. In addition, it is known [20] that any Gaussian Runge-Kutta scheme is both symplectic (Theorem 8.1, p. 99) and preserves quadratic invariants (Theorem 10.1, p. 136). The norm condition (6.1.3) is clearly quadratic, and the inextensibility condition (6.1.1) is also quadratic because the directors (3.16) – (3.18) are quadratic functions of the quaternion. The total linear impetus $\boldsymbol{X}^N$ (6.1.19) is actually linear in the state variables. Thus, amongst the invariants of motion only the Hamiltonian is not quadratic.

In the first instance we chose to implement the simplest Gaussian Runge-Kutta method, namely the midpoint method, which is a second-order integration scheme. For an ordinary differential equation of the form $\dot{\boldsymbol{z}} = \boldsymbol{f}(\boldsymbol{z})$, the midpoint method is

$$\boldsymbol{z}^{k+1} = \boldsymbol{z}^k + \tau \boldsymbol{f}\left(\frac{\boldsymbol{z}^{k+1} + \boldsymbol{z}^k}{2}\right) , \tag{6.2.1}$$

where τ is the time step, and $\boldsymbol{z}^k$ is the state at time $k\tau$. The midpoint method (6.2.1) is implicit, and must be solved iteratively. As a result, the quadratic invariants are in practice preserved only with the accuracy to which the implicit equation (6.2.1) is solved. For the purposes of the simulations presented here, it was sufficient to solve equation (6.2.1) by implementing a rather simple functional iteration scheme.

7 Results of Numerical Experiments

In this section we describe the results of some numerical simulations which were conducted using the algorithms outlined above. For the computations we chose the values of the material coefficients to be $\rho = 1$, $I_1 = 1 = I_2$, $I_3 = I_1 + I_2$, and $K_1 = 16 = K_2 = K_3$, and considered a rod of length 2π. These values of the coefficients were chosen purely for demonstration purposes, and have no associated units. Were one to choose values for these coefficients in MKS units corresponding to a thin metallic wire, the moments of inertia I_j would be rather small compared to both ρ and the bending stiffness K_j. One can think of the simulations presented here as corresponding to a set of nondimensionalized and scaled units of a realistic rod, in which the actual real time of the simulation is relatively short. In each case the rod spatial discretization was in sixty-four segments, so the dynamical system comprises 1024 ordinary differential equations. The time step used was

$\tau = 5 \cdot 10^{-3}$, and the duration of the simulation is 600, so the total number of time steps is 120,000. For the initial data taken in the Example 1 detailed below, the simulation includes more than thirty large amplitude oscillations. The iterative approximation to the solution of the midpoint method (6.2.1) was considered to have converged when the distance between successive approximations was less that $\epsilon = 10^{-11}$.

Our interest is in the calculation of the dynamics of large deformations of a rod. In Example 1, we consider a naturally straight, elastic rod and initially deform it to an untwisted circle, with zero initial velocities. In Figure 7.1 the first node, which is fixed, lies at the center of the figure on the left side of the initial circle, with the first segment pointing upward. While the initial configuration is closed, the final and initial segments of the rod are not connected, and Figure 7.1 depicts the ensuing motion when the rod is released. The configurations are shown as snapshots at equal time intervals, during which the rod moves in a generally counterclockwise direction. Figure 7.2 is a continuation of the evolution of the rod, with the first snapshot being the final state shown in Figure 7.1. During the second sequence the tip of the rod moves in a generally clockwise direction. Throughout the simulation the rod remains planar (as it should), although we actually compute a fully three-dimensional motion. As could have been expected, the motion is generally oscillatory, winding and unwinding from side to side, but the configuration does not come particularly close to resuming its initial circular shape. The elapsed time in Figures 7.1 and 7.2 together is 18 time units, so the entire simulation of 600 time units is the equivalent of approximately thirty-three oscillations.

Figure 7.3 shows the errors in the constraints for Example 1 over the full length of the simulation, i.e. a total number of 120,000 time steps. The broken curve represents the maximum error in $|\boldsymbol{q}^{n+\frac{1}{2}}|^2$ amongst all of the nodes, while the solid curve represents the maximum error in inextensibility amongst all of the segments. Because these constraints are quadratic functions of the state, the errors in the constraints are governed by the tolerance used in the solution of the implicit midpoint method at each time step, namely $\epsilon = 10^{-11}$. The accumulated error in the inextensibility condition is less than 0.6ϵ, while the accumulated error in the quaternion norm is less than 0.01ϵ.

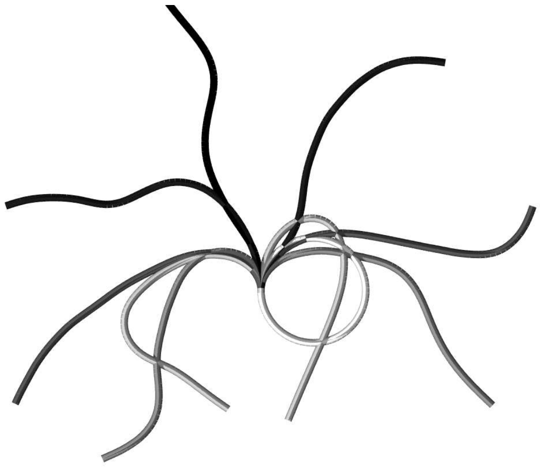

Figure 7.1: Snapshots of the motion of the rod in Example 1. Although the rod is initially circular in shape, the initial and final segments are not connected. The shading is used to code the sequence with the rod being white initially, becoming darker as the tip moves counterclockwise toward the top of the figure, and then becoming lighter again, until it is white in the last configuration which appears at the bottom left of the figure.

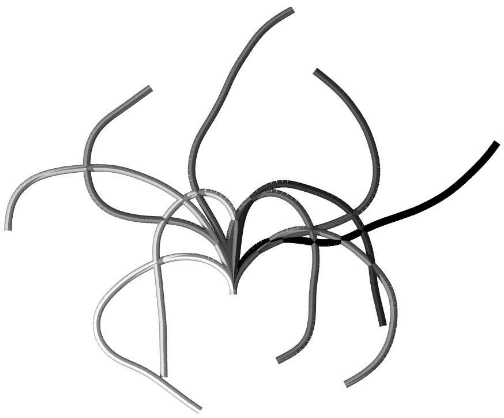

Figure 7.2: The motion of the rod in Example 1, continued. The same shading scheme is used as in Figure 7.1, with the overall motion being clockwise.

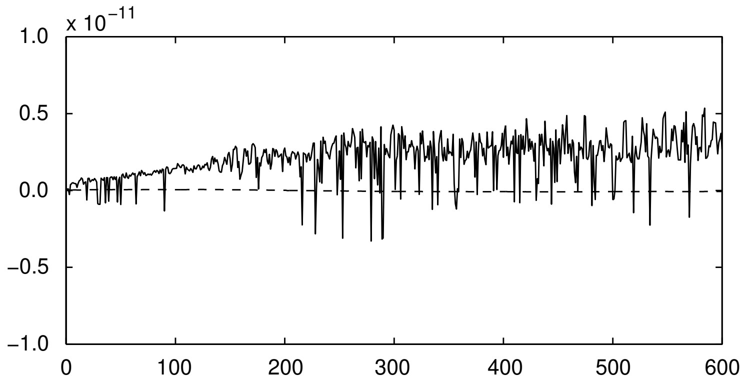

Figure 7.3: Errors in the constraints for the planar motion in Example 1. The accumulated error in the inextensibility condition (solid curve) is less than 0.6ϵ, where $\epsilon = 10^{-11}$ is the tolerance used in the solution of the implicit midpoint method at each time step. The accumulated error in the quaternion norm (broken curve) is less than 0.01ϵ.

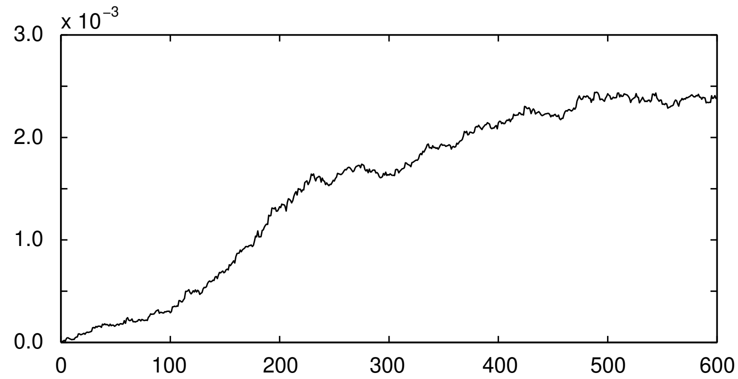

Figure 7.4: Relative error in the Hamiltonian for Example 1. The error at each integration step is proportional to τ^2, where $\tau = 5 \cdot 10^{-3}$ is the time step.

Figure 7.4 shows the relative error in the Hamiltonian for Example 1. The Hamiltonian H^N is not a quadratic function of the state. Therefore the error in H^N is proportional to $\tau^2 = 2.5 \cdot 10^{-5}$, the order of accuracy for the midpoint method. Note that the error in the constraints, although increasing, remains several orders of magnitude smaller than the error in the time-stepping scheme. We do not plot the errors in the total linear impetus (6.1.19) because the dynamics (6.1.16) imply that the linear impetus $\boldsymbol{\chi}^n$ is conserved *pointwise*. It follows that the total linear impetus $\boldsymbol{X}^N$ is *exactly* (i.e. to machine precision) constant throughout the time interval.

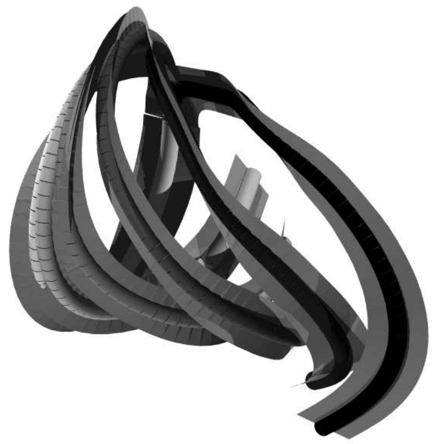

Figure 7.5: A sequence of snapshots depicting the three dimensional motion arising in Example 2. Here the centerline is initially colored white, and becomes darker as the evolution proceeds. The ribbon attached to the centerline of the rod indicates the twisting of the directors.

In Example 2, we consider the same initial circular configuration still with no initial velocities, but now with an additional uniform imposed twist corresponding to one complete rotation at the end. While the initial shape is planar, an unloading of the twist leads to highly nonplanar dynamics. The ensuing three-dimensional motions are much harder to illustrate effectively in snapshot figures, and movies can be found at the WWW site `http://jacobi.umd.edu/`.

Figure 7.5 shows the early evolution of the rod from its initial planar configuration. In this case there is significant coupling between the bending and twisting motions. Nevertheless, Figures 7.6 and 7.7 show that once again the norm condition, the inextensibility condition and the Hamiltonian are all preserved accurately by the time dynamics. As depicted in Figure 7.6 the maximum error in $|\boldsymbol{q}^{n+\frac{1}{2}}|^2$ (broken curve) is less than 0.3ϵ and the maximum error in inextensibility (solid curve) is less than 1.3ϵ after $120,000$ time steps, both significantly less than the discretization error associated with the solution. Figure 7.7 shows the relative error in the Hamiltonian for Example 2.

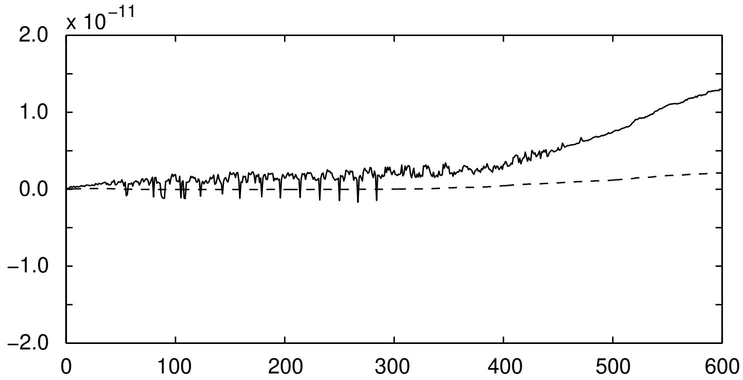

Figure 7.6: Errors in the constraints for the three-dimensional motion in Example 2. The accumulated error in the inextensibility condition (solid curve) is less than 1.3ϵ, where the tolerance ϵ is the same as in Example 1. The accumulated error in the quaternion norm (broken curve) is less than 0.3ϵ.

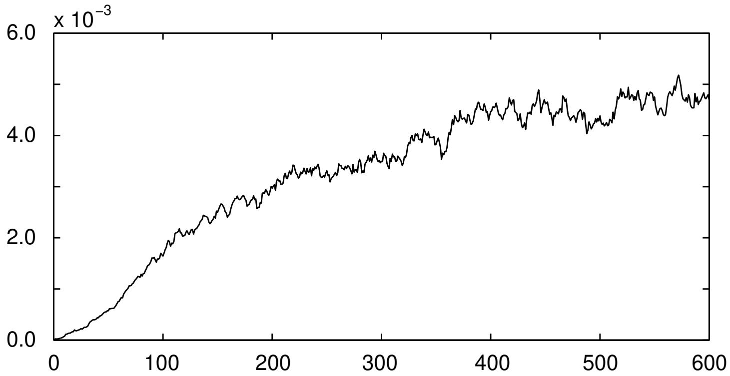

Figure 7.7: Relative error in the Hamiltonian for Example 2 is again proportional to τ^2 at each integration step, where the time step τ is the same as in Example 1.

Acknowledgements: It is a pleasure for the authors to thank Randy Paffenroth for assistance in the development of the graphics, and Dr. Joseph Sedlak of Computer Sciences Corporation, Professor R.B. Kellogg, Dr. Oscar Gonzalez, Dr. Rob Manning and Dr. Jian-Ming Xu for valuable contributions to this work.

References

[1] Antman, S.S. **Nonlinear Problems of Elasticity**. (Springer-Verlag, 1994).

[2] Arnold, V.I., V.V. Kozlov & A.I. Neishtadt. *Mathematical aspects of classical and celestial mechanics*, in **Dynamical Systems III, Encyclopædia of the Mathematical Sciences Volume 3**, ed. V.I. Arnold (Springer-Verlag, New York, 1988).

[3] Bottema, O. & B. Roth. **Theoretical Mechanics** (Dover, 1979).

[4] Brenan, K.E., S.L. Campbell & L.R. Petzold. Numerical Solution of Initial-Value Problems in Differential-Algebraic Equations. (SIAM, 1995).

[5] Charap, J.M., ed. **Geometry of Constrained Dynamical Systems** (Publications of the Newton Institute, Cambridge Press, 1995).

[6] Dichmann, D.J. Hamiltonian Dynamics of an Elastica and Stability of Solitary Waves. Ph. D. thesis, University of Maryland (1994).

[7] Dichmann, D.J, Y.W. Li & J.H. Maddocks. Hamiltonian formulations and Symmetries in Rod Mechanics. In *Mathematical Approaches to Biomolecular Structure and Dynamics*, J.P. Mesirov, K. Schulten & D.W. Sumners, eds., IMA Volumes in Mathematics and its Applications, **82** (Springer, New York, 1996), 71–113.

[8] Dichmann, D.J, J.H. Maddocks & R.L. Pego. Hamiltonian Dynamics of an Elastica and the Stability of Solitary Waves. *Arch. Rational Mech. Anal.* To appear.

[9] Dichmann, D.J, J.H. Maddocks & J.M. Xu. Three-Dimensional Hamiltonian Dynamics of an Elastica. In preparation.

[10] Dirac, P.A.M. On generalized Hamiltonian dynamics. *Can. J. Math.* **2** (1950) 129-148.

[11] Gonzalez, O. Mechanical Systems Subject to Holonomic Constraints: Differential Algebraic Formulations and Conservative Integration. *Physica D* submitted

[12] Gonzalez, O. & J.C. Simo. Exact Energy and Momentum Conserving Algorithms for General Models in Nonlinear Elasticity. *Comput. Meths. Appl. Mech. Engrg* submitted

[13] Junkins, J. & J. Turner. **Optimal Spacecraft Rotational Maneuvers** (Elsevier, 1986).

[14] Klapper, I. Biological Applications of the Dynamics of Twisted Elastic Rods. Journal of Computational Physics. To appear.

[15] Klein, F. & A. Sommerfeld. **Über die Theorie des Kriesels** (Johnson Reprint, 1965).

[16] Leimkuhler, B. & S. Reich. Symplectic integration of constrained Hamiltonian systems. Math. Comp. **63** (1994) 589–605.

[17] Leimkuhler, B. & R. Skeel. Symplectic numerical integrators in constrained Hamiltonian systems. J. Comp. Phys. **112** (1994) 117–125.

[18] Maddocks, J.H. & D.J. Dichmann. Conservation Laws in the Dynamics of Rods. *Journal of Elasticity.* **34** (1994) 83-96.

[19] Maddocks, J.H. & R.L. Pego. An unconstrained Hamiltonian formulation for incompressible fluid flow. *Comm. Math. Phys.* **170** (1995) 207–217.

[20] Sanz-Serna, J.M. and M.P. Calvo. **Numerical Hamiltonian Problems** (Chapman & Hall, 1994).

[21] Simo, J.C., N. Tarnow & M. Doblare. Nonlinear Dynamics of Three-Dimensional Rods: Exact Energy and Momentum Conserving Algorithms. *Intl. J. Numer. Methods Eng.* **38** (1995) 1431-1473.

[22] Simo, J.C. & L. Vu-Quoc. A Three-Dimensional Finite-Strain Rod Model. Part II: Computational Aspects. *Comput. Meths. Appl. Mech. Engrg* **58** (1986) 79-116.

[23] Simo, J.C. & L. Vu-Quoc. On the Dynamics in Space of Rods Undergoing Large Motions - A Geometrically Exact Approach *Comput. Meths. Appl. Mech. Engrg* **66** (1988) 125-161.

[24] Tabor, M. & Klapper, I.. Dynamics of Twist and Writhe and the Modeling of Bacterial Fibers. In *Mathematical Approaches to Biomolecular Structure and Dynamics*, J.P. Mesirov, K. Schulten & D.W. Sumners, eds., IMA Volumes in Mathematics and its Applications, **82** (Springer, New York, 1996), 139–160.